THE JOURNAL OF BIOLOGICAL CHEMISTRY VOL. 291, NO. 49, pp. 25462–25475, December 2, 2016
Published in the U.S.A.

Adaptor Protein CD2AP and L-type Lectin LMAN2 Regulate Exosome Cargo Protein Trafficking through the Golgi Complex*

Received for publication, March 24, 2016, and in revised form, September 27, 2016 Published, JBC Papers in Press, October 20, 2016, DOI 10.1074/jbc.M116.729202

Sang-Ho Kwon[‡1,2], **Sekyung Oh**[§¶1], **Marisa Nacke**[‖], **Keith E. Mostov**[‖], **and Joshua H. Lipschutz**[‡**]

From the [‡]*Department of Medicine, Division of Nephrology, Medical University of South Carolina, Charleston, South Carolina 29425, the* [§]*Department of Radiology, Stanford Cardiovascular Institute, and* [¶]*Department of Neurology and Neurological Sciences,Stanford University School of Medicine, Stanford, California 94305, the* [‖]*Departments of Anatomy and Biochemistry/Biophysics, University of California, San Francisco, California 94143, and the* **Department of Medicine, Ralph H. Johnson Veterans Affairs Medical Center, Charleston, South Carolina 29401*

Edited by Thomas Söllner

Exosomes, 40–150-nm extracellular vesicles, transport biological macromolecules that mediate intercellular communications. Although exosomes are known to originate from maturation of endosomes into multivesicular endosomes (also known as multivesicular bodies) with subsequent fusion of the multivesicular endosomes with the plasma membrane, it remains unclear how cargos are selected for exosomal release. Using an inducible expression system for the exosome cargo protein GPRC5B and following its trafficking trajectory, we show here that newly synthesized GPRC5B protein accumulates in the Golgi complex prior to its release into exosomes. The L-type lectin LMAN2 (also known as VIP36) appears to be specifically required for the accumulation of GPRC5B in the Golgi complex and restriction of GPRC5B transport along the exosomal pathway. This may occur due to interference with the adaptor protein GGA1-mediated trans Golgi network-to-endosome transport of GPRC5B. The adaptor protein CD2AP-mediated internalization following cell surface delivery appears to contribute to the Golgi accumulation of GPRC5B, possibly in parallel with biosynthetic/secretory trafficking from the endoplasmic reticulum. Our data thus reveal a Golgi-traversing pathway for exosomal release of the cargo protein GPRC5B in which CD2AP facilitates the entry and LMAN2 impedes the exit of the flux, respectively.

Vesicles found in extracellular fluids often carry biological information from the cells where they are released (1, 2). These extracellular vesicles play numerous roles in intercellular communication over a distance by delivering such macromolecules as pathogen-derived peptides on MHC proteins (3, 4); signaling molecules, including Wnt (5, 6), Hedgehog (7, 8), and growth factors and their receptors (9–11); and even genetic information in the forms of messenger RNAs and non-coding RNAs (12). When extracellular vesicles reach and are fused with the target cell membrane, the cargo molecules can elicit a variety of cellular responses ranging from activation of innate and adaptive immunity, body patterning, and stem cell regulation to tissue repair, tumorigenesis, and cancer metastasis (1, 2).

Sensing and responding to a wide variety of stimuli, the G-protein-coupled receptor (GPCR)[3] family proteins have traditionally been viewed as mediators of extracellular signals to cell-autonomous responses (13). Proteomics studies, however, have discovered a growing set of GPCR family proteins, including GPR179 (14), GPR155 (15), GPR100 (16), and GPRC5 family proteins (17), that are cargos of extracellular vesicles. This suggests that GPCR family proteins may also mediate intercellular communications when transported to target cells via extracellular vesicles. Although the biological roles of such non-cell-autonomous responses remain largely unexplored, our recent study has revealed that extracellular vesicle-mediated transport of the orphan G-protein-coupled receptor GPRC5B critically regulates three-dimensional tubule formation (18), assigning a new role for GPRC5B in addition to its previously reported cell-autonomous roles in mouse neocortex neurogenesis (19) and obesity-associated inflammatory signaling (20).

Cell biological approaches have revealed the basic mechanisms by which extracellular vesicles are generated and cargo molecules are loaded. On one hand, extracellular vesicles originate from a simple budding event of the plasma membrane, and the resulting vesicles are commonly called microvesicles

* This work was supported by a start-up package from the Medical University of South Carolina and an American Society of Nephrology Gottschalk Research Scholar grant (to S.-H. K.), National Institutes of Health Grants DK074398 and DK091530 (to K. E. M.) and DK074038 (to J. H. L.), and Veterans Affairs Merit Award 2I01BX000820 (to J. H. L.). The authors declare that they have no conflicts of interest with the contents of this article. The content is solely the responsibility of the authors and does not necessarily represent the official views of the National Institutes of Health.

[1] Both authors contributed equally to this work.

[2] To whom correspondence should be addressed: Dept. of Medicine, Medical University of South Carolina, 70 President St., Drug Discovery Bldg. Rm. 509, Charleston, SC 29425. Tel.: 843-876-2283; Fax: 843-879-5521; E-mail: kwonk@musc.edu.

[3] The abbreviations used are: GPCR, G-protein-coupled receptor; ESCRT, endosomal sorting complexes required for transport; HDR, homology-directed repair; ILVs, intraluminal vesicles; LH, left homologous region; MVEs, multivesicular endosomes; NLS, nuclear localization signal; RH, right homologous region; sgRNA, single guide RNA; S1P, sphingosine 1-phosphate; T2A, *T. asigna* virus 2A peptide; TGN, trans Golgi network; EHD, Eps15 homology domain; CRISPR, clustered regularly interspaced short palindromic repeats; AHSG, α2-HS-glycoprotein; Wls, Wntless; EGFP, enhanced GFP; FRT, Flp recombination target; DPBS, Dulbecco's PBS; ALIX, programmed cell death 6 interacting protein.

(also known as ectosomes) (1, 2). On the other hand, another type of extracellular vesicles, termed exosomes, appears to arise from complicated intracellular vesicular trafficking. It is known that exosome biogenesis begins with the formation of multivesicular endosomes (MVEs; also known as multivesicular bodies) (1, 2), which are characterized by harboring intraluminal vesicles (ILVs) that are derived from budding of the limiting endosomal membrane into the lumen of endosomes (21). It is thought that ILVs are released as exosomes when MVEs are fused with the plasma membrane (1, 2). Indeed, ILVs and exosomes display similar size and membrane lipid composition as well as the same membrane topology, supporting the view that exosomes originate from ILVs stored in MVEs (1, 2).

Recent reports have further provided insights into exosome biogenesis mechanisms. It is well appreciated that recognition of ubiquitinated cargo proteins on endosomal membrane by the endosomal sorting complexes required for transport (ESCRT) machinery ultimately leads to fusion of the MVEs with lysosomes rather than exosomal release (21, 22). Whereas some data suggest little involvement of ESCRT in targeting MVEs for exosomal release, other studies have demonstrated that the generation and release of exosomes containing such cargo proteins as Syndecan require PDCD6IP (also known as ALIX), which can bridge Syndecan to ESCRT-III complex (23). Thus, although the extent of ESCRT involvement remains unclear, release of at least some cargo proteins on exosomes appears to depend on ESCRT complexes. Conversely, it was shown that the exosomal membrane possesses a higher level of the lipid ceramide in the inner leaflet, which biophysically favors the small spherical shape of exosomes (24). An inhibitory G-protein-coupled receptor signaling, ensuing from engagement of the ceramide metabolite sphingosine 1-phosphate to its cognate receptors, was shown to mediate maturation of MVEs into the exosomes (25), suggesting an active role for ceramide and its derivatives in exosome biogenesis.

Although these studies established the role of MVEs in exosome biogenesis, how cargos are selected for exosomal release remains unclear. To address this issue, we investigated intracellular vesicle trafficking of the orphan G-protein-coupled receptor GPRC5B as a model exosome cargo protein (18). Although GPRC5B proteins are released in exosomes via a pathway relying on the GTPase activity of the exosome release regulator Rab35 (18, 26), a substantial fraction of GPRC5B proteins are also released in microvesicles along with other known exosome cargo proteins (18), complicating the mechanistic understanding of GPRC5B exosome loading. To circumvent this promiscuity, we focused our investigation on the early intracellular trafficking events of newly synthesized GPRC5B proteins. We show that most newly synthesized GPRC5B protein is released in exosomes as opposed to microvesicles and that an adaptor protein, CD2AP (27), mediates internalization of cell surface-localized GPRC5B as an early event. Surprisingly, we found that the internalized GPRC5B proteins subsequently accumulated in the Golgi complex prior to exosomal release and that the L-type lectin LMAN2 (28, 29) impedes the exosomal release of GPRC5B specifically from the trans Golgi network (TGN), possibly by interfering with the physical association of GPRC5B and GGA1, an adaptor protein implicated in TGN-to-endosome trafficking (30, 31), or possibly by opposing the biosynthetic secretory trafficking through TGN-to-endoplasmic reticulum (ER) retrograde transport (28). Thus, the exosomal cargo protein GPRC5B may move along a trafficking route through the Golgi compartment, controlled by an LMAN2-mediated inhibition of the flux.

Results

An Inducible Expression System to Study GPRC5B Trafficking and Release on Exosomes—To better understand the mechanism of exosome biogenesis and GPRC5B trafficking, we utilized a doxycycline-inducible expression system in HEK293 cells. We engineered a C-terminally HA-tagged GPRC5B protein (GPRC5B-HA) to be expressed from a chromatin context in response to doxycycline, which relieves tet repressor-mediated blockade of GPRC5B-HA transcription (Fig. 1*A*). Exosomes were prepared from cultured cell medium with sequential differential centrifugation in combination with polymer-based precipitation (32), which resulted in specific enrichment of known exosome cargo proteins Flotillin-1 (33) and CD63 (34) in the exosome fraction as revealed by Western blotting analysis (Fig. 1*B*). Using these methods of inducible expression and exosome preparation, we first noted that exosome release of GPRC5B-HA is tightly regulated by doxycycline in our cultured cell system with GPRC5B-HA being barely detectable in exosome fractions in the absence of doxycycline and the level increasing in response to doxycycline over time, first becoming detectable at 60 min after doxycycline addition and gradually accumulating thereafter (Fig. 1*C*). Consistent with our previous report using a GFP-tagged GPRC5B (GPRC5B-GFP) (18), GPRC5B-HA in the exosome fraction was resolved by SDS-PAGE as a doublet (Fig. 1*C*). The slower migrating band appears to correspond to a glycosylated form as deglycosylating enzyme treatment made both GPRC5B-GFP forms revolve as a faster migrating singlet (Fig. 1*D*). These data suggest that both GPRC5B-HA and GPRC5B-GFP undergo normal post-translational modifications and confirm that both forms of GPRC5B proteins are released in exosomes.

Our previous study showed that a substantial fraction of GPRC5B-GFP protein can be released in microvesicles in addition to exosomes but is not detected in apoptotic bodies (18). In fact, according to the ExoCarta database (35), many known exosome cargo proteins are also found in microvesicles, complicating studies on exosome cargo loading mechanisms. These observations, however, were largely based on experimental systems that captured a steady state profile of extracellular vesicles. We reasoned that our temporally inducible system for GPRC5B-HA expression might help us distinguish GPRC5B-HA loading to exosomes from that to microvesicles. Indeed, when GPRC5B-HA expression was induced for 3 h, 92% of GPRC5B-HA protein released in extracellular vesicles was recovered from the exosome fraction, whereas only 8% was found in the microvesicle fraction (Fig. 1*E*). Hence, our inducible expression system enabled us to focus our investigation on exosomal release mechanisms of GPRC5B-HA protein using a short time expression ($\leq$3 h).

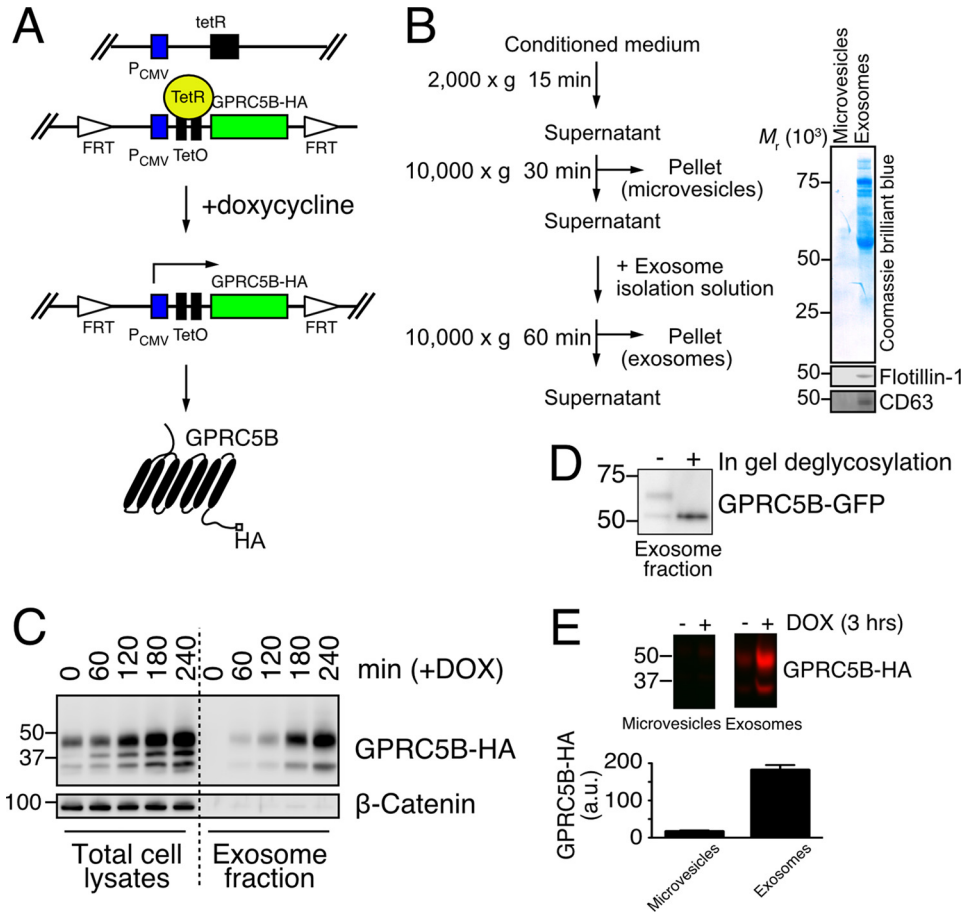

FIGURE 1. **An inducible expression system to study GPRC5B trafficking and release on exosomes.** *A*, schematic diagram showing doxycycline-mediated expression of a C-terminally HA-tagged GPRC5B (GPRC5B-HA) from HEK293 Flp-In T-REx cells that harbor a tetracycline-inducible GPRC5B-HA expression cassette in a chromatin context. *B*, *left*, the exosome preparation strategy from conditioned medium using sequential differential centrifugation in combination with polymer-based exosome precipitation (32). *Right*, representative exosome and microvesicle fractions as revealed by SDS-PAGE and Coomassie Brilliant Blue staining (*top*) and exosome marker (Flotillin-1 and CD64) Western blotting analysis (*bottom*). *Numbers* to the *left* of SDS-polyacrylamide gels in this and all subsequent figures represent relative molecular masses ($M_r \times 10^3$). *C*, Western blot analysis for GPRC5B-HA protein detected in the exosome fraction in response to doxycycline. Expression and exosomal release levels are proportional to the time (min) after doxycycline addition. +*DOX* represents doxycycline addition in this and all subsequent figures. 10% of cells were used to prepare total cell lysates for comparison with those of the exosome fraction in this and all subsequent figures. *D*, in-gel deglycosylation assay reveals that the slower migrating band of the doublet GPRC5B-GFP protein in exosome fractions corresponds to a glycosylated form. *E*, Western blotting analysis for GPRC5B-HA proteins after fractionation of extracellular vesicles into microvesicle and exosome fractions. When expression is induced for 3 h with doxycycline (+*DOX*), the majority of GPRC5B-HA protein (92%) partitions into the exosome fraction. *Top*, near-infrared fluorescence detection of GPRC5B-HA proteins using an anti-HA antibody in microvesicle and exosome fractions with (+) or without (−) doxycycline (*DOX*) induction. *Bottom*, quantitation of the Western blotting analysis. *Error bars* represent S.E. *TetR*, tet repressor; *a.u.*, arbitrary unit.

An RNAi Candidate-based Screen for Regulators of Exosomal Release of GPRC5B—Using our inducible GPRC5B-HA expression system, we searched for regulatory factors that are critical for exosome loading. Proteins mediating exosome biogenesis can themselves be released on exosomes as reported for Rab35, Syntenin, and Flotillin-1 (23, 26, 36). We thus focused on exosome components found in human urine (15) and tested their requirements for GPRC5B-HA exosomal release by knocking down their expression using small interfering RNA (siRNA).

PDCD6IP (also known as ALIX) is known to mediate exosome biogenesis at the level of intraluminal budding of endosomal membranes (23) and is found in human urinary exosomes (15). We noted that knockdown of PDCD6IP resulted in a significant decrease of GPRC5B-HA in the exosome fraction (Fig. 2), confirming the requirement of PDCD6IP for exosome biogenesis (23, 37) and demonstrating the utility of our siRNA-mediated knockdown screening strategy that focused on urinary exosome components.

Extending siRNA-mediated knockdown to other human urinary exosome components, we identified additional factors required for exosomal release of GPRC5B, including IST1, EHD1, and EHD4 of which siRNA-mediated knockdowns all resulted in a significant decrease of GPRC5B levels in exosomes (Fig. 2). IST1 is a known component of ESCRT-III complexes and is involved in the processes of cytokinesis and nuclear envelope reformation (22). EHD1 and EHD4 are members of the Eps15 homology domain (EHD) family proteins, which play key roles in various endosome transport processes (38).

We further identified another positive regulator of GPRC5B exosomal release, CD2AP. CD2AP has not been previously linked to exosome biogenesis. siRNA-mediated knockdown of CD2AP expression significantly decreased the level of GPRC5B-HA in exosomes (Fig. 2). CD2AP has been implicated in endocytosis by acting as an adapter protein between membrane proteins and the actin cytoskeleton (27). Our screening also uncovered a novel regulator that appears to inhibit exo-

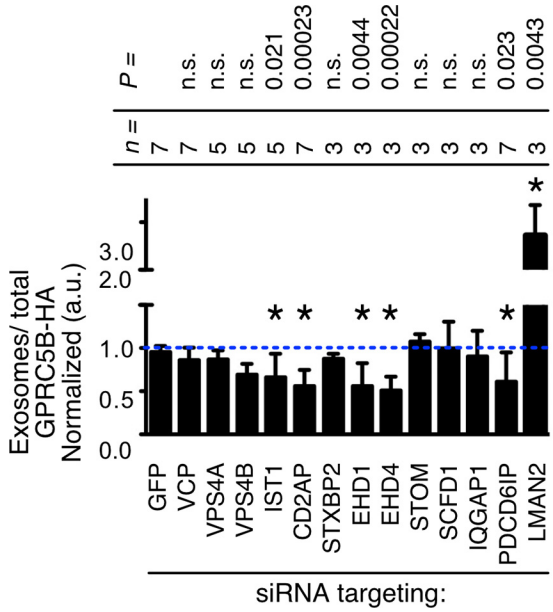

FIGURE 2. **A candidate-based RNAi screen for regulators of exosomal release of GPRC5B.** The effect of siRNA-mediated knockdown of human urinary exosome components on exosome release of GPRC5B-HA is shown. The *blue dotted line* indicates exosomal GPRC5B-HA from cells transfected with the siRNA targeting GFP, which served as a negative control. Knockdown of PDCD6IP was used as a positive control, resulting in a reduction of GPRC5B-HA in the exosome fraction. Data are shown as mean ± S.D. (*error bars*). *, $p < 0.05$ (considered statistically significant) as measured by Student's *t* test comparing data from each siRNA target with data of siRNA targeting GFP from at least three independent experiments. *n.s.*, not significant; *a.u.*, absorbance units; *VCP*, valosin-containing protein; *STOM*, stomatin.

TABLE 1
List of siRNAs that significantly affected exosomal release of GPRC5B-HA

Target genes	Sequences (5′ to 3′)	Notes
PDCD6IP	aag agc tgt gtg ttg ttc aat	Positive control
IST1	tcg cct taa act att gga gaa	
IST1	aaa gtt tgt ctt gac agt tga	
CD2AP	tac gat gta taa ttt acc taa	KD1 in Fig. 3
CD2AP	ttg cac tat agg agt cat aaa	KD2 in Fig. 3
EHD1	atg ccc aat gtc ttt ggt aaa	
EHD1	ttg agc aat aag aaa cca gaa	
EHD4	caa gat caa gct cga cgg cta	
LMAN2	agc ggg agc att cgc tca tta	

somal release of GPRC5B-HA. Knockdown of LMAN2 (also known as VIP36) resulted in a substantial increase of GPRC5B-HA in exosomes (Fig. 2). LMAN2 is thought to play a critical role in vesicle trafficking by acting as an L-type lectin (28, 29). This suggests that LMAN2 may inhibit exosomal release of GPRC5B by controlling the trafficking of vesicles containing exosome cargo proteins. To our knowledge, LMAN2 represents the first reported case of a negative regulator of exosome cargo loading. Given these results, we set out to investigate the roles of CD2AP and LMAN2 in intracellular trafficking and exosome loading of GPRC5B as both proteins have been previously implicated in vesicle trafficking (27–29) but not in exosome biogenesis or exosome cargo loading.

CD2AP Mediates Targeting of GPRC5B to Perinuclear Puncta during Exosome Loading—To confirm a role for CD2AP in GPRC5B exosomal release, we tested two distinct siRNAs targeting CD2AP (Table 1, KD1 and KD2) for their ability to alter GPRC5B exosomal release. We found that both siRNAs substantially reduced exosomal GPRC5B-HA levels, whereas they did not significantly alter intracellular GPRC5B-HA levels (Fig. 3*A*). Notably, this appears to result from specific targeting by the CD2AP siRNAs, as opposed to an off-target effect, as the normal exosomal level of GPRC5B-HA was restored when a GFP-tagged mouse *Cd2ap*, which is not recognizable by our siRNAs against human CD2AP, was co-transfected with the human CD2AP KD1 siRNA (Fig. 3*A*).

To better understand the role of CD2AP in exosome loading of GPRC5B, we generated a loss of function allele of the *CD2AP* gene in HEK293 cells that harbor the inducible GPRC5B-HA expression construct. We prepared a targeting vector containing sequences of *mKate* (encoding a far-red fluorescence protein) and *pac* (encoding a puromycin *N*-acetyltransferase) genes in tandem that are separated by the ribosome-skipping *Thosea asigna* virus 2A peptide (T2A) (39, 40) for bicistronic expression (mKate-T2A-PuroR) (Fig. 3*B*). The *mKate* sequence used in this study lacked the translation start codon (ATG) to allow mKate-T2A-PuroR to be expressed from the transcriptional and translational controls of the endogenous *CD2AP* gene (Fig. 3*B*). This expression cassette was inserted into the genome via homology-directed repair (HDR) with a Cas9/CRISPR-mediated double strand break (41, 42) of the flanking sequences of exon 2 of the *CD2AP* gene (Fig. 3*B*). *CD2AP* exon 1 is composed entirely of 5′-untranslated region (5′-UTR) and the translation-initiating methionine codon (ATG) at its 3′-end. The successful replacement of *CD2AP* exon 2 with the mKate-T2A-PuroR cassette is thus expected to produce a transcript that has an open reading frame of the mKate-T2A-PuroR cassette that is directly fused 3′ to the CD2AP 5′-UTR. The remainder of the *CD2AP* coding sequence would be untranslatable due to translation termination at the end of the mKate-T2A-PuroR cassette and the lack of translation reinitiation signals 3′ to the cassette. Hence, our strategy for precise genome editing for *CD2AP* knock-out is that only in-frame insertion of the template into the target site allows the mKate fluorescent protein and the puromycin resistance gene to be expressed from the endogenous *CD2AP* promoter in the genome. Western blotting analysis of PuroR$^+$ mKate$^+$ double positive clones confirmed inactivation of the *CD2AP* gene by our HDR strategy, and CD2AP protein expression was not detected in homozygous *CD2AP*-null (*CD2AP*$^{-/-}$) cells (Fig. 3*B*).

Consistent with siRNA-mediated knockdown results (Figs. 2 and 3*A*), exosomes prepared from *CD2AP*$^{-/-}$ cell culture by polymer-based exosome precipitation (32) contained substantially less GPRC5B-HA protein when expressed for 3 h than those from wild-type cells (Fig. 3*C*). To exclude the possibility that the effect of the short term induction of GPRC5B might only reflect a perturbation to the biosynthetic trafficking pathway before the steady state is reached, we also prepared exosomes at 24 h post-GPRC5B-HA induction and again found a much reduced level of GPRC5B-HA proteins in exosomes released from *CD2AP*$^{-/-}$ cells (Fig. 3, *C* and *D*). Because the polymer-based exosome preparation might precipitate other extracellular vesicles, we alternatively prepared exosomes from *CD2AP*$^{-/-}$ cells using ultracentrifugation of the postmicrovesicle fraction (18). This method also identified less

GPRC5B-HA protein in exosomes prepared from *CD2AP*$^{-/-}$ cells than in those from wild-type cells (Fig. 3*E*), thus ruling out the possibility of inadequate or inappropriate recovery of GPRC5B-HA proteins by our choice of exosome collection methods. This also confirmed the requirement of CD2AP for GPRC5B-HA exosomal release.

We next examined intracellular localization of the newly synthesized GPRC5B-HA protein. Wild-type cells accumulated GPRC5B-HA proteins at 1.2 h after doxycycline addition in perinuclear punctate structures, whereas GPRC5B-HA expressed in *CD2AP*$^{-/-}$ cells accumulated mainly near or at the cell surface (Fig. 3*F*). Importantly, the punctate structures containing GPRC5B-HA were almost undetectable in *CD2AP*$^{-/-}$ cells (Fig. 3*F*). When mouse *Cd2ap* was exogenously expressed in *CD2AP*$^{-/-}$ cells, GPRC5B-HA protein was redistributed to the punctate structures as seen in wild-type control cells (Fig. 3*G*). These results demonstrated that CD2AP is necessary for accumulation of GPRC5B in the perinuclear punctate structures.

A Fraction of GPRC5B Proteins Is Internalized from the Cell Surface and Accumulates in the TGN Prior to Exosomal Release—Given the known role of CD2AP as an adaptor in endocytosis (27) and the appearance of the punctate localiza-

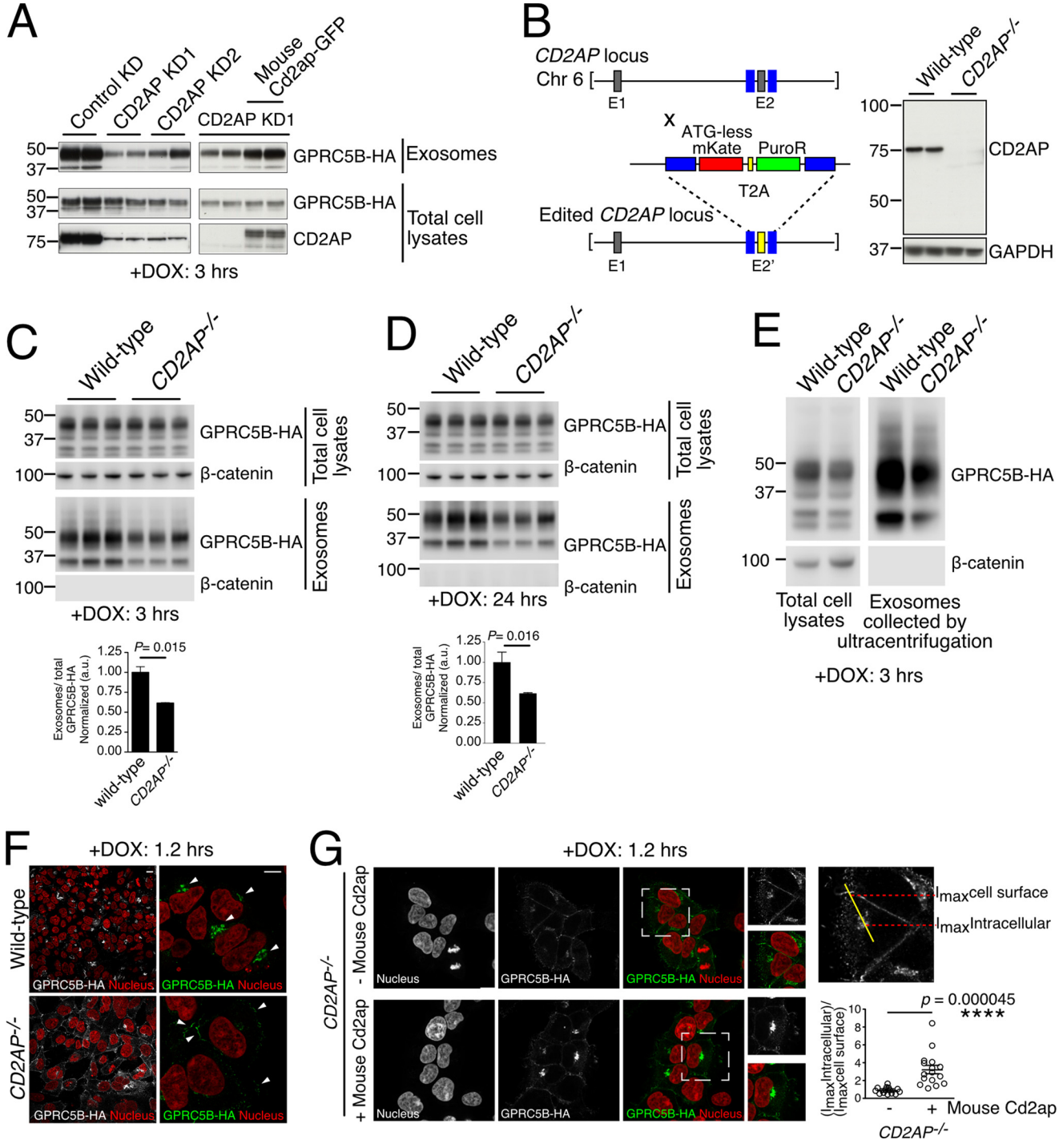

tion of GPRC5B-HA as early as at 1.2 h after expression induction, it is possible that GPRC5B proteins are internalized from the cell surface for their subsequent loading into exosomes. Indeed, when we labeled cell surface-localized proteins with biotin following 3 h of GPRC5B-HA expression and subsequently chased the resulting biotinylated cell surface proteins, the level of biotinylated GPRC5B-HA proteins in the exosomal fraction increased over time (Fig. 4*A*). These data indicate that at least a fraction of exosomal GPRC5B proteins originated from the cell surface. Using the same labeling protocol combined with subcellular fractionation in a sucrose gradient, biotinylated GPRC5B-HA protein was recovered from intracellular fractions that also contained RCAS1 (also known as EBAG9), a Golgi-resident protein (43), at 30 min after cell surface labeling (Fig. 4*B*), demonstrating that GPRC5B proteins are internalized from the cell surface, which likely occurs prior to their release into exosomes. Our data, however, do not rule out the additional possibility that newly synthesized GPRC5B-HA protein might accumulate at the punctate structures during its trafficking through the biosynthetic secretory pathway. Of note, a substantial fraction of GPRC5B-HA protein is still detectable in exosomes even when the *CD2AP* gene is completely inactivated (Fig. 3, *C–E*), suggesting that another mechanism, possibly involving the biosynthetic/secretory pathway, may work in parallel with CD2AP-dependent internalization of cell surface-localized GPRC5B-HA protein for exosomal release.

The punctate structures containing GPRC5B may be a crucial hub for vesicle trafficking of exosome cargo proteins. A recent study demonstrated that signaling following sphingosine 1-phosphate (S1P) binding to its cognate receptors and the consequent activation of the inhibitory G-protein (G_i) plays a critical role in maturation of MVEs for exosome release (25). We thus examined S1P receptor localization in our cells and indeed found that two isoforms of S1P receptor, S1P1 (isoform 1) and S1P3 (isoform 3), co-localized with GPRC5B-HA at the perinuclear puncta (Fig. 4*C*). This suggests that the punctate structures are conducive for sorting of exosome cargo proteins, such as GPRC5B.

Given the perinuclear distribution of GPRC5B-HA as well as the co-fractionation of GPRC5B-HA with the Golgi marker RCAS1 (43) (Fig. 4*B*), we asked whether this structure corresponds to the Golgi complex. When cells were co-stained with GM130 (a marker for the cis/medial Golgi) or TGN46 (a marker for trans Golgi), respectively, we indeed observed a significant co-localization of GPRC5B-HA with these markers but much less, if any, with the late endolysosomal markers LAMP1 and LAMP2 (Fig. 4*D*). Because many compartments, including late endosomes, can be concentrated in the perinuclear region, we treated cells with the microtubule-disrupting agent nocodazole to better resolve the GPRC5B-HA-containing puncta. We again found significant co-segregation of GPRC5B-HA with GM130 (Fig. 4*E*). We extended our analysis to another exosome cargo protein, AHSG (also known as Fetuin-A), a recently identified exosome biomarker for acute kidney injury (44), and observed that a V5-tagged AHSG protein (AHSG-V5) also co-localized with the TGN marker TGN46 as well as with GPRC5B-HA (Fig. 4*F*). Taken together, these data demonstrate that the Golgi complex, including TGN, is a major site where exosome cargo proteins, such as GPRC5B and AHSG, reside during intracellular trafficking.

LMAN2 Opposes GPRC5B Trafficking in the Exosomal Release Pathway at the TGN—We next considered the role of LMAN2 in exosome loading of GPRC5B. Importantly, it is in the Golgi complex where the type I transmembrane L-type lectin LMAN2 is thought to control vesicle trafficking (28, 29). The striking increase in exosomal GPRC5B-HA expression following knockdown of LMAN2 expression (Fig. 2) may thus be a consequence of altered trafficking of GPRC5B through the Golgi complex. We therefore first examined the localization of LMAN2 when GPRC5B-HA expression was induced. Notably, LMAN2 and GPRC5B-HA were found to accumulate together in the Golgi complex, including TGN (Fig. 4, *C–E*), suggesting a role for LMAN2 in GPRC5B trafficking and exosomal release at the level of the Golgi complex, including the TGN.

To better define the role of LMAN2, we generated a loss of function allele of *LMAN2* in a cell line that also harbors the doxycycline-inducible GPRC5B-HA construct using error-prone non-homologous end joining repair near the 5′-end of the coding sequence of the *LMAN2* gene (Fig. 5*A*) with a CRISPR/Cas9-mediated double strand break (41, 42). Unlike *CD2AP*, we were unable to obtain cells that were homozygous null for *LMAN2* (Fig. 5*A*). The resulting heterozygous *LMAN2*$^{+/-}$ cells, however, expressed a substantially reduced level of LMAN2 protein as determined by Western blotting

FIGURE 3. **CD2AP mediates targeting of GPRC5B to the perinuclear puncta during exosome loading.** *A*, specific requirement of CD2AP homologs in mediating exosomal release of GPRC5B as revealed by Western blotting analysis. *Left*, two distinct siRNAs (KD1 and KD2) targeting CD2AP both decrease GPRC5B-HA protein levels in exosome fractions. *Right*, restoration of GPRC5B-HA exosomal release by expression of a GFP-tagged mouse *Cd2ap* (Cd2ap-GFP) in cells co-transfected with a siRNA (KD2) targeting human CD2AP. *B*, *left*, strategy for *CD2AP*$^{-/-}$ cell generation by Cas9/CRISPR-mediated genome editing. HDR utilizing the sequences (*blue*) flanking exon 2 (*E2*) of the *CD2AP* gene replaces exon 2 with an ATG-less mKate-T2A-PuroR cassette (altered to *E2′*). *Right*, Western blotting analysis confirms the loss of CD2AP expression in *CD2AP*$^{-/-}$ cells. GAPDH is a loading control. *C–E*, Western blotting analyses of total cell lysates and exosome fractions of wild-type and *CD2AP*$^{-/-}$ cells after 3 (*C* and *E*) and 24 h (*D*) of doxycycline (*DOX*)-mediated GPRC5B-HA expression. Exosomes were prepared by polymer-based precipitation (*C* and *D*) (32) or by ultracentrifugation of the postmicrovesicle fraction (*E*) (18). *C* and *D*, *bottom*, quantitative analyses of chemiluminescence signals from nitrocellulose membranes. Note the decreased GPRC5B-HA protein level in exosomes from *CD2AP*$^{-/-}$ cells. *, $p < 0.05$. *F*, loss of CD2AP expression alters intracellular localization of GPRC5B-HA proteins, which were induced with doxycycline for 1.2 h. GPRC5B-HA proteins in wild-type cells localized to cytoplasmic puncta as revealed by immunofluorescence microscopy stained with anti-HA antibody. *CD2AP*$^{-/-}$ cells, in contrast, instead accumulate GPRC5B-HA proteins at or near the plasma membrane. The *left* and *right columns* show low and high magnifications, respectively. Similar results were obtained from 3-h induction experiments (not shown). *Scale bar*, 10 μm. *G*, restoration of cytoplasmic punctum localization of GPRC5B-HA protein following exogenous expression of mouse *Cd2ap* in *CD2AP*$^{-/-}$ cells as seen by immunofluorescence microscopy stained with anti-HA antibody. *Scale bar*, 10 μm. *Top right*, fluorescence intensity ratio was calculated by measuring maximum GPRC5B-HA fluorescence intensity from the cell surface (I_{max}(cell surface)) and intracellular signals (I_{max}(intracellular)) along a *yellow line* as shown in *CD2AP*$^{-/-}$ cells. *Bottom right*, ratio of I_{max}(cell surface) and I_{max}(intracellular) was quantified for statistical analysis. Data are shown as mean ± S.E. (*error bars*). ****, $p < 0.0001$ (considered statistically significant) as measured by Student's *t* test. *E1*, exon 1; *a.u.*, arbitrary unit.

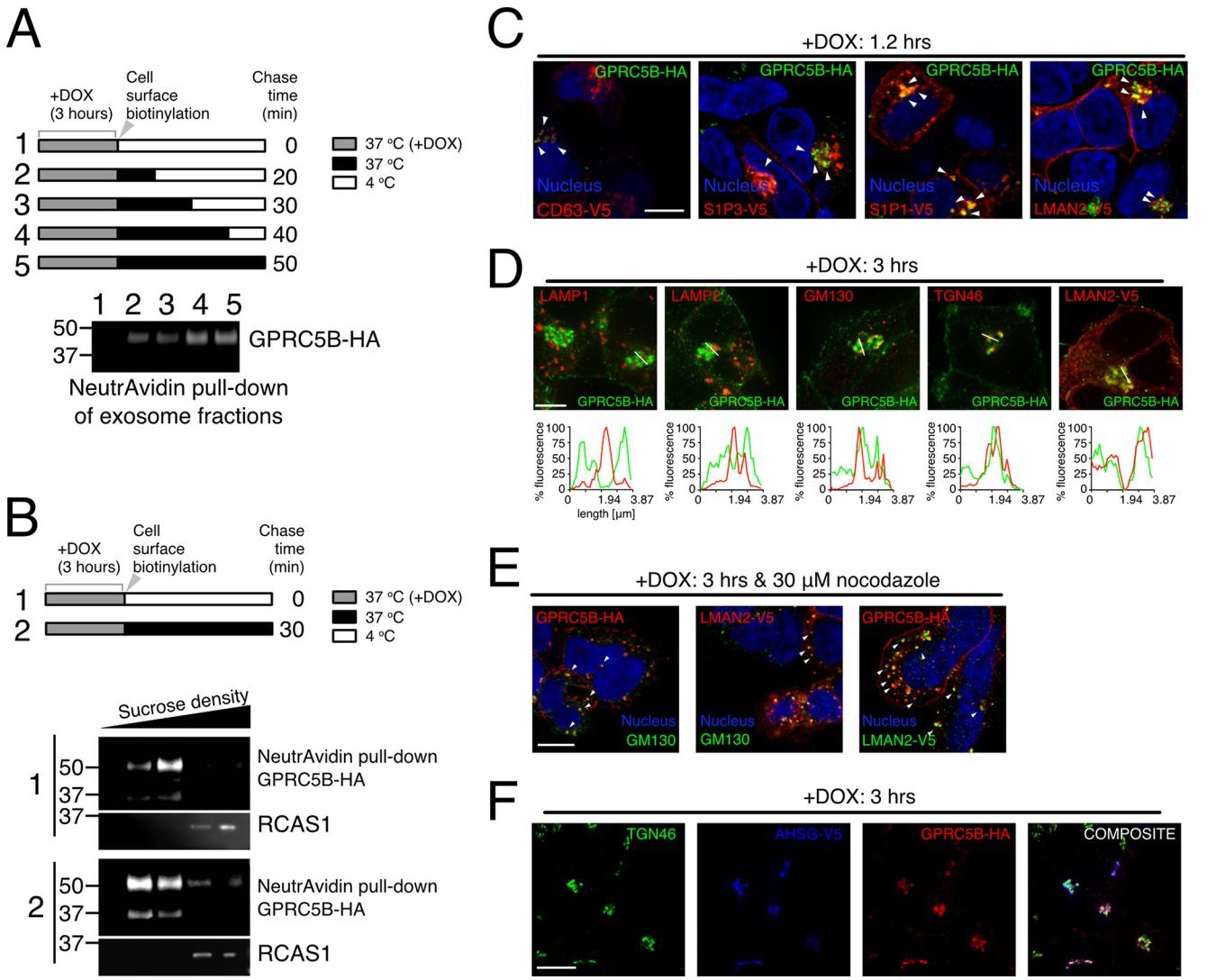

FIGURE 4. **GPRC5B accumulates in the Golgi complex during exosome loading.** *A*, Western blotting analysis of NeutrAvidin-purified proteins in exosome fractions. Cells were treated with doxycycline for GPRC5B-HA expression (+*DOX*; 3 h) followed by a cell surface biotinylation pulse and chasing by incubating at 37 °C for variable times. Note that the level of NeutrAvidin-purified GPRC5B-HA proteins increases with 37 °C chase time. *B*, Western blotting analysis of NeutrAvidin-purified proteins in fractions of a sucrose gradient ultracentrifugation. Cells were treated with doxycycline for GPRC5B-HA expression (+*DOX*; 3 h) followed by cell surface biotinylation and subsequent incubation at 37 °C for either 0 or 30 min. Note the appearance of NeutrAvidin-purified GPRC5B-HA protein that co-segregates with the Golgi-resident protein RCAS1 at 30 min of 37 °C incubation after cell surface biotinylation. *C*, GPRC5B-HA protein, expressed after induction with doxycycline for 1.2 h, co-localizes with V5-tagged S1P receptors S1P1 (isoform 1) and S1P3 (isoform 3), and the V5-tagged L-type lectin LMAN2 (LAMN2-V5) as revealed by immunofluorescence microscopy. *Arrowheads*, co-localization. *Scale bar*, 10 μm. *D*, high degree of co-localization of GPRC5B-HA proteins with the Golgi markers GM130 and TGN4, as well as with LMAN2-V5 but less or no co-localization with late endolysosomal markers LAMP1 and LAMP2 as observed by immunofluorescence microscopy. *Scale bar*, 10 μm. Percent pixel intensities of fluorescence signals along *white lines* in the *upper* micrographs were plotted in the *bottom* graphs. *E*, co-localization of GPRC5B-HA and LMAN2-V5 with the Golgi marker GM130 in nocodazole-treated cells. *Arrowheads*, co-localization. *Scale bar*, 10 μm. *F*, another exosome cargo protein, AHSG, co-localizes with the TGN marker TGN46 together with GPRC5B-HA as revealed by immunofluorescence microscopy. *Scale bar*, 10 μm.

analysis (Fig. 5*A*) and were therefore used in the subsequent experiments.

To examine the role of LMAN2 in exosome release of GPRC5B, we induced GPRC5B-HA expression with doxycycline in *LMAN2*$^{+/-}$ cells. We found that the exosomal GPRC5B-HA level was significantly increased in exosomes prepared by polymer-based precipitation (32) from *LMAN2*$^{+/-}$ cells when compared with exosomes prepared from wild-type cells (Fig. 5*B*). When collected after 24 h of GPRC5B-HA expression, exosomes released from *LMAN2*$^{+/-}$ cells still contained significantly more GPRC5B-HA protein than those from wild-type cells (Fig. 5*C*), suggesting that the effect of *LMAN2* gene dosage on exosomal release of GPRC5B is unlikely to be due to perturbation of the biosynthetic trafficking pathway, which can potentially be associated with short term expression (<3 h). Exosomes prepared by ultracentrifugation of the post-microvesicle fraction (18) from *LMAN2*$^{+/-}$ cells also displayed more GPRC5B-HA protein than those from wild-type cells (Fig. 5*D*). In contrast, overexpression of a V5-tagged LMAN2 construct (LMAN2-V5) in wild-type cells significantly reduced exosomal GPRC5B-HA levels (Fig. 5*E*). Furthermore, expression of LMAN2-V5 in *LMAN2*$^{+/-}$ cells suppressed exosome release of GPRC5B-HA to the level found in wild-type control cells that overexpress LMAN2-V5 (Fig. 5*E*). Taken together, these observations indicate that LMAN2 plays a critical role in inhibiting exosome loading of cargo proteins, such as GPRC5B.

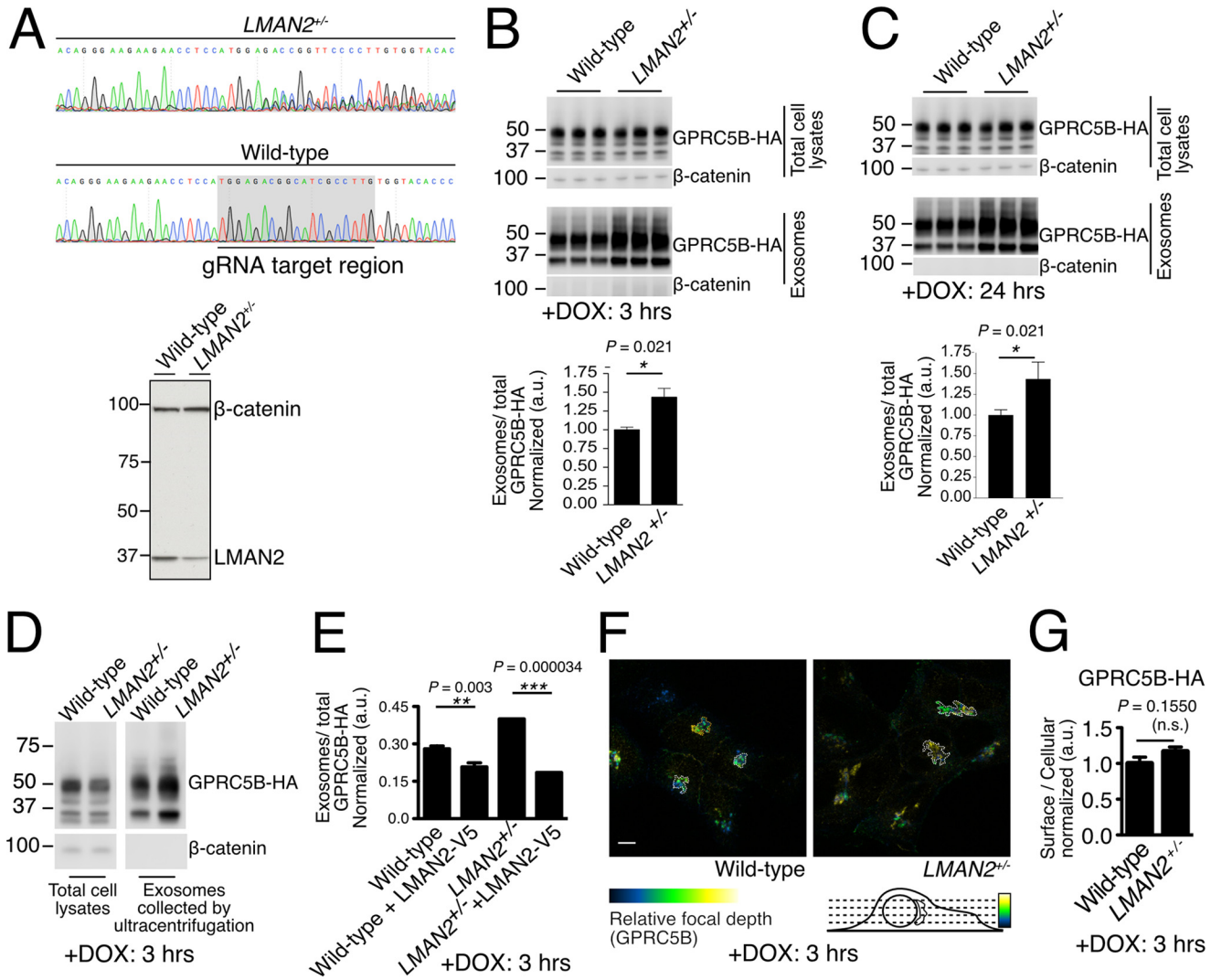
A
LMAN2+/-
Wild-type
gRNA target region
Wild-type
LMAN2+/-
100
75
50
37
β-catenin
LMAN2
B
Wild-type
LMAN2+/-
50
37
100
GPRC5B-HA
β-catenin
Total cell lysates
Exosomes
+DOX: 3 hrs
P = 0.021
*
Exosomes/ total GPRC5B-HA Normalized (a.u.)
1.75
1.50
1.25
1.00
0.75
0.50
0.25
0.00
Wild-type
LMAN2 +/-
C
Wild-type
LMAN2+/-
50
37
100
GPRC5B-HA
β-catenin
Total cell lysates
Exosomes
+DOX: 24 hrs
P = 0.021
*
Exosomes/ total GPRC5B-HA Normalized (a.u.)
1.75
1.50
1.25
1.00
0.75
0.50
0.25
0.00
Wild-type
LMAN2 +/-

D
Wild-type
LMAN2+/-
Wild-type
LMAN2+/-
75
50
37
100
GPRC5B-HA
β-catenin
Total cell lysates
Exosomes collected by ultracentrifugation
+DOX: 3 hrs
E
P = 0.000034
P = 0.003
**
***
Exosomes/ total GPRC5B-HA Normalized (a.u.)
0.45
0.30
0.15
0.0
Wild-type
Wild-type + LMAN2-V5
LMAN2+/-
LMAN2+/- +LMAN2-V5
+DOX: 3 hrs
F
Wild-type
LMAN2+/-
Relative focal depth (GPRC5B)
+DOX: 3 hrs
G
GPRC5B-HA
P = 0.1550
(n.s.)
Surface / Cellular normalized (a.u.)
1.5
1.0
0.5
0.0
Wild-type
LMAN2+/-
+DOX: 3 hrs

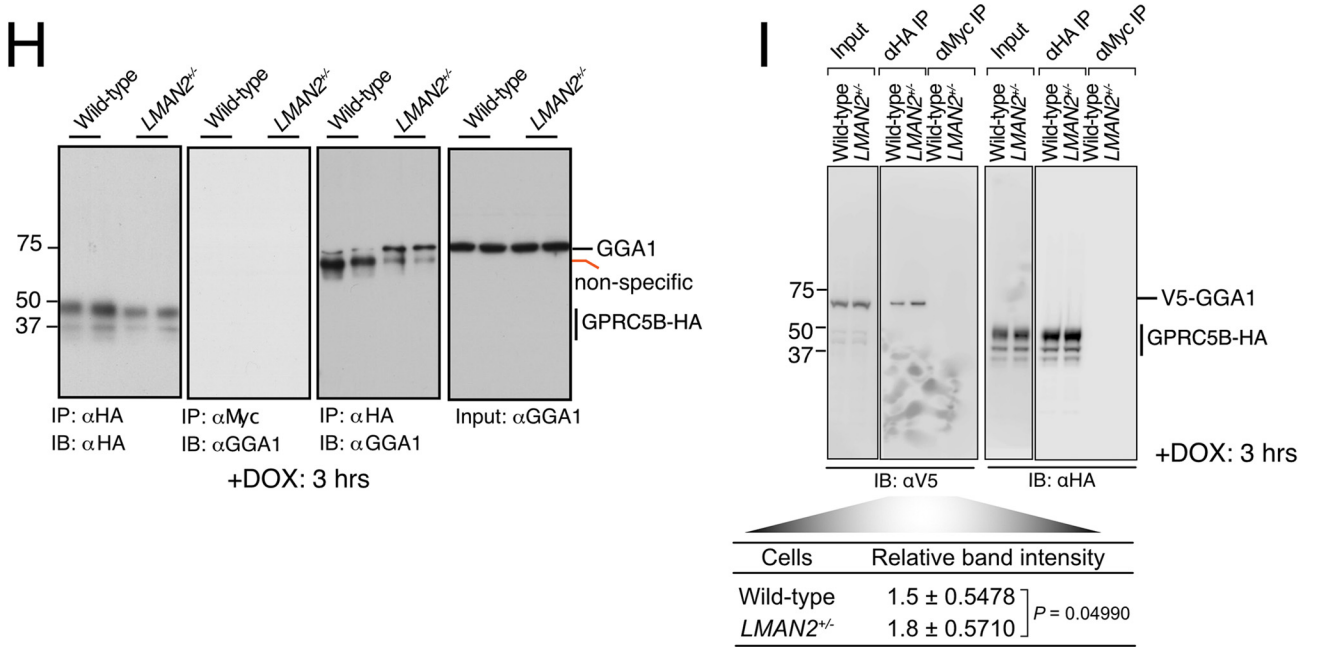
H
Wild-type
LMAN2+/-
Wild-type
LMAN2+/-
Wild-type
LMAN2+/-
Wild-type
LMAN2+/-
75
50
37
GGA1
non-specific
GPRC5B-HA
IP: αHA
IB: αHA
IP: αMyc
IB: αGGA1
IP: αHA
IB: αGGA1
Input: αGGA1
+DOX: 3 hrs
I
Input
αHA IP
αMyc IP
Input
αHA IP
αMyc IP
Wild-type
LMAN2+/-
75
50
37
V5-GGA1
GPRC5B-HA
IB: αV5
IB: αHA
+DOX: 3 hrs
Cells
Relative band intensity
Wild-type
1.5 ± 0.5478
LMAN2+/-
1.8 ± 0.5710
P = 0.04990

Given the co-localization of GPRC5B and LMAN2 in the Golgi complex, including TGN (Fig. 4, *D* and *E*), LMAN2 may limit GPRC5B exosome loading by specifically regulating trafficking in the TGN or other Golgi compartments. In support of this, GPRC5B-HA protein expressed in *LMAN2*$^{+/-}$ cells was found to be more dispersed than the Golgi-localized GPRC5B-HA in wild-type cells (Fig. 5*F*, compare the areas surrounded by *dotted lines*). The increased LMAN2 protein level in exosomes released from *LMAN2*$^{+/-}$ cells does not appear to be associated with the level of GPRC5B-HA protein at the plasma membrane as revealed by Western blotting analysis of GPRC5B-HA protein biotinylated at the cell surface (Fig. 5*G*). These data thus suggest that LMAN2 is specifically required for limiting GPRC5B trafficking in the Golgi complex for exosome release but does not affect GPRC5B trafficking to the plasma membrane.

The dispersed GPRC5B localization in *LMAN2*$^{+/-}$ cells (Fig. 5*F*) suggests that LMAN2 may restrict exosome cargo sorting and/or budding from the TGN or other Golgi compartments. To test this, we investigated GGA1, an adaptor protein that is implicated in vesicle trafficking from the TGN to endosomes by promoting AP-1-coated vesicle budding from the TGN (30, 31). We found that both endogenous GGA1 (Fig. 5*H*) and V5 epitope-tagged GGA1 (V5-GGA1) (Fig. 5*I*) associated with GPRC5B-HA as revealed by Western blotting analysis following co-immunoprecipitation (Fig. 5, *H* and *I*). Notably, the interaction of GPRC5B-HA with either endogenous GGA1 (Fig. 5*H*) or V5 epitope-tagged GGA1 (Fig. 5*I*) was enhanced in *LMAN2*$^{+/-}$ cells (Fig. 5, *H* and *I*), raising the possibility that LMAN2 controls GPRC5B sorting and budding from the TGN compartment by opposing the interaction between GPRC5B and GGA1.

Discussion

Recent studies have shown that exosome biogenesis involves the formation of endosomes and their subsequent maturation into MVEs and that ILVs stored in MVEs are released as exosomes (1, 2). Given the dynamic nature of endosome trafficking (21), however, it has remained unclear how exactly exosome cargo proteins are loaded into MVEs. We addressed this question by using an inducible expression system for the exosome cargo protein GPRC5B (18) and following its intracellular localization toward exosomal release. We focused on early trafficking pathways, through which newly synthesized GPRC5B proteins are loaded and released in exosomes, to minimize secondary complications, such as their release into microvesicles. Importantly, our analyses revealed a novel role for the Golgi compartments, including the TGN, in exosome trafficking.

Our inducible expression system demonstrated that endocytosis critically contributes to exosomal release of cargo proteins, including GPRC5B. We identified the adaptor protein CD2AP as a novel regulator in this early step of exosome biogenesis as indicated by the accumulation of GPRC5B at or near the plasma membrane in the absence of CD2AP (Fig. 3). Recent studies showed that CD2AP binds to an ESCRT-III complex component, PDCD6IP (also known as ALIX) (45, 46). Because both CD2AP (this study) and PDCD6IP (this study (Fig. 2) and Ref. 23) are required for exosome biogenesis and physically interact with each other (45, 46), they may well cooperate to release a common set of cargo molecules into exosomes.

The ablation of CD2AP expression resulted in accumulation of GPRC5B at or near the plasma membrane and, importantly, concurrent disappearance of GPRC5B from the Golgi complex (Fig. 3, *F* and *G*). This suggests that retrograde trafficking from the plasma membrane and/or endosomes to the Golgi complex follows initial CD2AP-dependent trafficking during the biogenesis of GPRC5B-containing exosomes. However, given that complete inactivation of *CD2AP* still allows for GPRC5B exosomal release (Fig. 3), we do not rule out an additional trafficking route that the Golgi accumulation may also reflect a time-dependent accumulation of newly synthesized GPRC5B protein in the Golgi apparatus during its movement through the biosynthetic secretory pathway from the ER to the plasma membrane. These two possibilities are not mutually exclusive, and exosome cargo proteins, such as GPRC5B, may be carried along two parallel routes, namely 1) the retrograde plasma membrane-to-Golgi route and 2) the biosynthetic ER-to-Golgi route. The co-localization of the TGN marker TGN46 and exosome cargo proteins AHSG and GPRC5B (Fig. 4) highlights the importance of the TGN in exosome cargo protein trafficking irrespective of which vesicle trafficking route is used for exosomal cargo release.

Our data reveal a regulatory mechanism by which Golgi-accumulated GPRC5B protein moves toward exosomal release. We showed that the L-type lectin LMAN2 restricts exosomal release of GPRC5B from the Golgi complex by limiting the

FIGURE 5. **LMAN2 limits GPRC5B exosome loading by opposing GGA1-mediated GPRC5B trafficking from the TGN.** *A*, *top*, Sanger sequencing of the Cas9/CRISPR-targeted *LMAN2* locus. Mixed signals in the *upper* sequencing track indicate heterozygous status (*LMAN2*$^{+/-}$) of the *LMAN2* locus targeted by the *LMAN2*-specific single guide RNA (*gRNA*). *Bottom*, Western blotting analysis showing the reduction of LMAN2 protein production in the *LMAN2*$^{+/-}$ cells. β-Catenin is a loading control. *B–D*, Western blotting analyses of total cell lysates and exosome fractions of wild-type and *LMAN2*$^{+/-}$ cells after 3 (*B* and *D*) and 24 h (*C*) of doxycycline (*DOX*)-mediated GPRC5B-HA expression induction. Exosomes were prepared by polymer-based precipitation (*B* and *C*) (32) or by ultracentrifugation of the postmicrovesicle fraction (*D*) (18). *B* and *C*, *bottom*, quantitative analyses of chemiluminescence signals from nitrocellulose membranes. Note the increased GPRC5B-HA protein in exosomes from *LMAN2*$^{+/-}$ cells. *E*, expression of LMAN2-V5 in both wild-type and *LMAN2*$^{+/-}$ cells reduces GPRC5B-HA protein levels in exosome fractions as determined by quantitation of Western blotting analysis. *F*, localization of GPRC5B-HA in *LMAN2*$^{+/-}$ cells is more dispersed from the TGN than that it is in wild-type control cells as revealed by immunofluorescence microscopy stained with anti-HA antibody. A series of *z*-axis images around the Golgi marker TGN46 was captured to determine the localization of GPRC5B-HA at or around the Golgi complex. Projection images are from the *z*-series of confocal images, which are individually pseudo-colored with the indicated colors. The areas with the GPRC5B-HA signals above the threshold from the projection images are marked with a *dotted line* to help visualize more dispersed distribution of GPRC5B-HA in *LMAN2*$^{+/-}$ cells compared with wild-type control cells. *Scale bar*, 10 μm. *G*, cell surface levels of GPRC5B-HA proteins in *LMAN2*$^{+/-}$ cells and in control wild-type cells are not significantly (*n.s.*) different as determined by quantitation of Western blotting analysis. *H* and *I*, GPRC5B-HA proteins participate in a molecular complex either with endogenous GGA1 (*H*) or with exogenously expressed V5-GGA1 (*I*) as revealed by co-immunoprecipitation. Note the enhanced level of interaction in *LMAN2*$^{+/-}$ cells compared with wild-type control cells. *a.u.*, absorbance units; *IP*, immunoprecipitation; *IB*, immunoblotting.

interaction of GPRC5B with the adaptor protein GGA1. GGA1 has been previously implicated in the TGN-to-endosome trafficking (30, 31) (Fig. 5, *H* and *I*). Our findings thus suggest that a trafficking route, regulated by LMAN2 and GGA1, for generating MVEs from the TGN contributes to the loading and releasing of cargo proteins, such as GPRC5B, into exosomes.

How can endocytosed exosome cargo proteins reach the Golgi complex prior to their release in exosomes? A number of studies have established that a protein complex, termed the retromer, mediates the endosome-to-Golgi route of trafficking (47–49). Notably, we identified two Eps15 homology proteins, EHD1 and EHD4, as factors needed for GPRC5B exosomal release in our siRNA screen (Fig. 2). Of note, understanding how these proteins contribute to GPRC5B exosomal release would require further experimental validation. However, EHD1 is known to interact with the retromer components VPS26 and VPS35 to retrieve the mannose 6-phosphate receptor from the plasma membrane and transport it to the TGN (50–52). This suggests that endosome-to-TGN trafficking via the retromer pathway can result in accumulation of internalized GPRC5B proteins at the TGN prior to exosomal release. Retromer-dependent trafficking to the TGN compartment could account for secretion of other exosome cargos, such as the Wnt-releasing factor Wntless (Wls; also known as Evi) (6, 53). Wls was shown to move from the plasma membrane to the TGN via the retromer pathway (5, 6, 54–58). Although this retromer-mediated Wls retrieval was interpreted as a recycling mechanism for its reuse in Wnt secretion (5, 6), it is also consistent, according to our data, with the idea that Wls traffics from the plasma membrane to the TGN and then is released on exosomes.

Our findings shed light on the mechanisms of vesicle trafficking for exosome cargo loading and release (Fig. 6). Exosome cargo trafficking is initiated with internalization of cargo proteins, such as GPRC5B, through modulation of the actin cytoskeleton by CD2AP (Fig. 6). The resulting endosomes transfer their content to the TGN and other Golgi compartments, possibly in a retromer-dependent manner (Fig. 6). GGA1-dependent TGN/Golgi-to-endosome trafficking, which is restricted by LMAN2, then may move the exosome cargo proteins to endosomes and maturing MVEs for their release on exosomes (Fig. 6).

Given that LMAN2 was shown to mediate Golgi-to-ER retrograde trafficking (28), it may also reduce the flux of newly synthesized GPRC5B proteins through opposing the biosynthetic/secretory trafficking from the ER (Fig. 6). This possibility is also consistent with our observation of the dispersed GPRC5B-HA staining around the Golgi complex associated with the reduced LMAN2 levels (Fig. 5*F*). No matter how LMAN2 controls this retrograde Golgi-to-ER trafficking, the fact that loss of CD2AP-mediated internalization does not completely abolish GPRC5B exosomal release (Fig. 3) suggests involvement of alternative trafficking routes, such as the biosynthetic/secretory pathway from the ER to the Golgi (Fig. 6).

Of note, LMAN2 is also known to be shed into the extracellular space from the plasma membrane, which is required for subsequent phagocytosis (59), suggesting another alternative

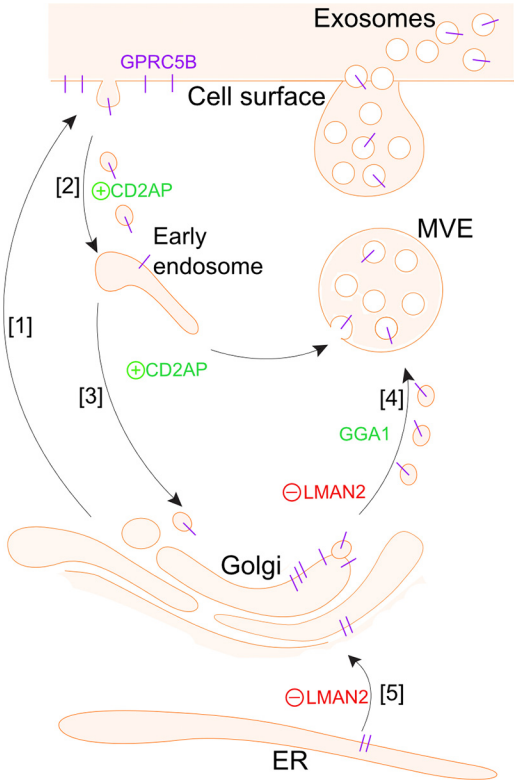

FIGURE 6. **Possible model for exosomal release of GPRC5B.** Following delivery to the cell surface (*1*), GPRC5B (*purple*) is internalized (*2*) and/or recycled to the Golgi complex in a CD2AP-dependent manner (*3*). At the Golgi complex, LMAN2 limits GGA1-dependent trafficking of GPRC5B to the MVEs destined for exosome formation (*4*). Reducing LMAN2 levels facilitates loading of GPRC5B on the GGA1-dependent route from the TGN (*5*), leading to increased exosomal release of GPRC5B. In parallel with the CD2AP-mediated internalization pathway, GPRC5B may also accumulate at the Golgi complex during the biosynthetic secretory trafficking from ER (*5*). LMAN2 may also inhibit GPRC5B exosomal release by mediating Golgi-to-ER retrograde transport (28), opposing the biosynthetic secretory trafficking (*5*).

possibility that LMAN2 can limit the extracellular GPRC5B level through the recapturing of GPRC5B-containing extracellular vesicles and subsequent internalization. Nevertheless, our data support the idea that LMAN2 acts inside cells to mediate GPRC5B exosomal release given that we did not observe a significant difference in cell surface levels of GPRC5B proteins between cells that differ in *LMAN2* gene dosage (Fig. 5*G*).

Our discovery of exosome cargo protein trafficking through the TGN/Golgi raises a crucial question: whether and how can cargo proteins of the canonical biosynthetic ER-Golgi-plasma membrane secretory pathway and those of the exosome pathway be differentially recognized and selectively sorted in the TGN? Interestingly, we observed the signature of active S1P receptor signaling in the GPRC5B-containing TGN/Golgi compartment (Fig. 4*A*), suggesting that S1P receptor signaling can serve to distinguish exosome cargo proteins from those in the biosynthetic secretory pathway at the TGN/Golgi, extending its previously implicated role in exosome cargo sorting in MVEs (25). Regardless of an S1P receptor signaling role, the TGN/Golgi may also promote or permit critical post-translational modifications of exosome cargo proteins, such as phosphorylation, glycosylation, ubiquitination, and acetylation, for their selective and faithful release in exosomes. Future studies

addressing this issue will lead to a better understanding of exosome cargo selection and vesicle trafficking.

Experimental Procedures

Plasmids—To construct an inducible expression construct for GPRC5B, the open reading frame (ORF) of canine GPRC5B was PCR-amplified with a C-terminal HA epitope tag using pEGFP-N1-GPRC5B as a template (18). The PCR product was subcloned by using Gibson Assembly (60) into pcDNA5/FRT/TO (Invitrogen) that had been linearized by HindIII and XhoI. The resulting plasmid was named pcDNA5/FRT/TO-GPRC5B-HA. Expression of the GPRC5B-HA fusion coding sequence is under the control of a tetracycline-regulated promoter ($tetO_2$-CMV).

For generating single guide RNA (sgRNA)-expressing vectors, a synthetic DNA fragment composed of the U6 promoter, target sequence-guide RNA scaffold, and transcription terminator in tandem was subcloned into pCR-BluntII-TOPO (Invitrogen) using Zero Blunt TOPO reaction. After testing the cleavage efficiency of three different sgRNAs per target gene with the Surveyor mutation detection kit (Transgenomics), the following target sequences were chosen to establish genome-edited cell lines: for *CD2AP* editing, GAATGTGAAAAAGCTACAGG, and for *LMAN2* editing, ACAAGGCGATGCCGTCTCCA.

To construct a donor plasmid for *CD2AP* editing via HDR, a bicistronic vector containing sequences of *3xNLS-mKate* encoding a far-red fluorescence protein fused with an N-terminal triple nuclear localization signal (NLS) and *pac* (encoding a puromycin *N*-acetyl transferase) genes in tandem that are separated by the ribosome-skipping peptide T2A (3xNLS-mKate-T2A-PuroR; a gift from Dr. Luke M. Judge at the J. David Gladstone Institute). The construct was first mutagenized by using Gibson Assembly (60) to remove a 675-bp (3608–4282) fragment containing the triple NLS and the start codon of the mKate fluorescence protein. The resulting plasmid was named as HDR donor-ATG-less mKate-2A-puro. An ~700-bp flanking region around the target site in exon 2 of the *CD2AP* gene was sequenced by using genomic DNA that had been obtained from HEK293 T-REx cells. Using the sequencing result, 282-bp 5′ upstream (left homologous region (LH)) and 3′ downstream (right homologous region (RH)) sequences flanking the HDR target site were each chemically synthesized. Using Gibson Assembly (60), these synthetic fragments were subcloned into HDR donor-ATG-less mKate-2A-puro, generating the *CD2AP* HDR donor plasmid with a promoterless expression cassette (LH-ATG-less mKate-2A-puro-RH).

All V5 epitope-tagged expression plasmids used in this study were obtained from DNASU. pCas9-GFP and hCas9 were obtained from Addgene. For rescue experiments, pEGFP-N1-mouse Cd2ap (obtained from Andrey Shaw's laboratory; expressing C-terminally EGFP-tagged mouse *Cd2ap* homolog) was mutagenized to generate an untagged Cd2ap expression vector by introducing a stop codon at the end of the coding sequence of mouse *Cd2ap*. The siRNA sequences targeting human *CD2AP* do not match the coding sequence of mouse *Cd2ap* in the mutagenized pEGFP-N1-mouse Cd2ap. All constructs were verified by automated Sanger DNA sequencing.

Cell Lines—Flp-In T-REx HEK293 cells (Invitrogen) were maintained in DMEM (Gibco; containing high glucose and GlutaMAX) supplemented with 10% (v/v) Tet System Approved fetal bovine serum (Clontech), 100 units/ml penicillin, 100 mg/ml streptomycin, 100 μg/ml Zeocin, and 15 μg/ml blasticidin S and humidified in 5% CO_2 at 37 °C. Cells were passaged at subconfluence and routinely checked for *Mycoplasma* contamination.

To generate cell lines harboring a doxycycline-inducible GPRC5B-HA cassette, Flp-In T-REx HEK293 cells were transfected with pcDNA5/FRT/TO-GPRC5B-HA as well as pOG44 (Invitrogen) encoding a Flp recombinase (61). Cells with genomic integration of GPRC5B-HA through Flp/FRT-mediated recombination were selected with 100 μg/ml hygromycin B (Sigma) for 2 weeks (61). Cells with successful genomic integration of pcDNA5/FRT/TO-GPRC5B-HA at the FRT landing site were tested for sensitivity to 100 μg/ml Zeocin (Sigma) and maintained in DMEM (containing high glucose and GlutaMAX) supplemented with 10% Tet System Approved fetal bovine serum (Clontech), 100 units/ml penicillin, 100 mg/ml streptomycin, 15 μg/ml blasticidin S, and 100 μg/ml hygromycin B (61). GPRC5B-HA expression was routinely induced in this cell line by adding 1 μg/ml doxycycline hyclate (Sigma).

For the *CD2AP* knock-out line, the Flp-In T-REx HEK293 cells harboring the inducible GPRC5B-HA expression cassette at an FRT site were co-transfected with three plasmids, pCR-BluntII-TOPO expressing sgRNA targeting *CD2AP*, an hCas9 expression plasmid, and LH-ATG-less mKate-2A-puro-RH, using Turbofector (Thermo Scientific). Only in-frame insertion of the template in the designated target site allows the mKate fluorescent protein and the puromycin resistance gene to be expressed from the endogenous *CD2AP* promoter, discriminating it from random integration of the two selective markers. 32 h after transfection, cells were selected with 1 μg/ml puromycin (Sigma) for 2 weeks. From pooled puromycin-resistant colonies, mKate-positive cells were sorted into 96-well plates, each well receiving equal to or less than one cell, to clone cells with complete inactivation of endogenous *CD2AP* expression by our HDR-mediated insertional mutagenesis.

For generating *LMAN2* indel mutations, Flp-In T-REx HEK293 cells harboring the inducible GPRC5B-HA expression cassette were co-transfected with pCR-BluntII-TOPO expressing sgRNA targeting *LMAN2* and a plasmid expressing pCas9-GFP. 32 h after transfection, GFP-positive cells were sorted into 96-well plates, each well receiving equal to or less than one cell. Sorted single cell clones were propagated, and their genomic DNA was extracted using the QuickExtract DNA extraction kit (Epicenter). A1591-bp region flanking the *LMAN2* target site was PCR-amplified using Q5 High-Fidelity DNA polymerase (New England Biolabs) and the following primers: CACTCCCGTGATGTCAATGC (forward) and GGCCAGAACATTTAGGGGTC (reverse). The resulting PCR fragments were subjected to automated Sanger DNA sequencing to determine the presence of an indel mutation.

Exosome Preparation—3 h before preparation, growth medium was replaced by serum-free medium, and conditioned medium was collected and centrifuged at 2000 × *g* for 15 min and 10,000 × *g* for 20 min. The resulting pellets correspond to

the microvesicle fraction. Exosomes were subsequently prepared using two different methods. First, the supernatants were combined with 0.5 volume of Total Exosome Isolation reagent (Invitrogen) and mixed by vortexing. After incubation at 4 °C for 18–20 h, the mixture was centrifuged at 10,000 × *g* for 1.5 h at 4 °C, and the supernatant was removed. Second, alternatively, the postmicrovesicle supernatants were spun at 100,000 × *g* for 1 h and 15 min (18). The resulting exosome pellets were resuspended either with Laemmli sample buffer supplemented with 50 mM β-mercaptoethanol for Western blotting analysis or 20 mM sodium phosphate (pH 7.2), 150 mM NaCl, 1 mM EDTA, 10% glycerol, 1% Triton X-100, and Complete Mini protease inhibitor mixture (Roche Applied Science) for biotin-NeutrAvidin pulldown assays.

Exosome Release Screen with siRNA-mediated Knockdown—Predesigned siRNAs targeting human genes were purchased from Qiagen or Ambion. Transfection of control or the indicated siRNAs was performed according to the manufacturers' instructions. Briefly, 24 h before transfection, 2.4×10^5 cells were plated into 24-well plates coated with poly-L-lysine hydrobromide (Sigma). Annealed siRNAs (final concentration, 7 nM) were transfected using HiPerfect (Qiagen). 48 h after transfection, GPRC5B-HA expression was induced for 3 h with 1 μg/ml doxycycline in 300 μl of serum-free growth medium. Collected conditioned media from 2 wells per sample were combined for exosome preparation. Total lysates were also prepared for calculating exosome release efficiency ($\text{GPRC5B-HA}_{\text{exosomes}}/\text{GPRC5B-HA}_{\text{cellular}}$).

Antibodies—Primary antibodies used were rat anti-HA (Roche Applied Science), mouse anti-V5 (Invitrogen), goat anti-V5 (Abcam), mouse anti-GAPDH (Millipore), sheep anti-TGN46 (AbD Serotec), mouse anti-GM130 (BD Biosciences), mouse anti-LAMP1 (Developmental Studies Hybridoma Bank), mouse anti-LAMP2 (Developmental Studies Hybridoma Bank), rabbit anti-CD2AP (Santa Cruz Biotechnology), rabbit anti-LMAN2 (Sigma), rabbit anti-GGA1 (Thermo Scientific), rabbit anti-CD63 (Santa Cruz Biotechnology), mouse anti-Flotillin-1 (BD Biosciences), anti-RCAS1 (Cell Signaling Technology), and rabbit anti-β-catenin (Santa Cruz Biotechnology). Secondary antibodies used were Alexa Fluor 555-conjugated anti-mouse, Alexa Fluor 555-conjugated anti-rabbit, Alexa Fluor 488-conjugated anti-mouse, Alexa Fluor 488-conjugated anti-rabbit, Alexa Fluor 647-conjugated anti-mouse, and Alexa Fluor 647-conjugated anti-rabbit (Invitrogen) and HRP-conjugated anti-mouse, HRP-conjugated anti-rabbit, and HRP-conjugated anti-goat (Jackson).

Immunofluorescence Microscopy and Quantitative Image Analysis—5×10^3–10^4 cells were grown on coverslips or Chambered Coverglass (8-wells; Lab Tek II) coated with poly-L-lysine hydrobromide (Sigma). Cells were washed twice with DPBS (+calcium, +magnesium), fixed for 20 min with 4% paraformaldehyde (Affymetrix), and blocked/permeabilized with PFS buffer (0.7% fish skin gelatin, 0.025% saponin, 0.01% sodium azide in DPBS) for at least 2 h sequentially. The indicated primary antibodies were incubated in PFS buffer at 4 °C overnight. After extensive washing with PFS buffer, samples were incubated with fluorescence-conjugated secondary antibodies in PFS buffer. Nuclei were stained with Hoechst 33342 (Invitrogen). Samples were subsequently washed with DPBS and then mounted using ProLong Gold Antifade (Invitrogen). For experiments in Fig. 4*C*, 3 h after induction of GPRC5B-HA with 1 μg/ml doxycycline, cells were treated with 30 μM nocodazole (Sigma) for 2 h. For confocal microscopy, digital images were taken with either an LSM 510 META NLO microscope (Zeiss); a TCS SP5 microscope (Leica) equipped with laser modules of 488, 564, and 633 nm and a two-photon laser; or a Cell Observer Spinning Disc confocal microscope (Zeiss) equipped with a three-laser module (405, 488, and 561 nm) using a Plan-Apochromat 63×/1.40 numerical aperture oil lens. Images were processed using ImageJ (National Institutes of Health). A fluorescence intensity trace along the indicated line was generated by the plot profile function in ImageJ. The degree of co-localization was determined with object Pearson's correlation coefficients using Huygens version 3.6 (Scientific Volume Imaging) to distinguish the average pixel values of two channels from background.

Sucrose Density Gradient Centrifugation—Cells were homogenized in Golgi isolation buffer (Sigma) supplemented with protease inhibitors (Roche Applied Science) using a polytetrafluoroethylene pestle, and the homogenates were spun at 3000 × *g* for 15 min at 4 °C. 2.3 M sucrose solution was added to the postnuclear supernatants to make a final concentration of 1.25 M sucrose. The samples were then further fractionated over four discontinuous step gradients (1.84, 1.25, 1.1, and 0.25 M) by centrifuging at 120,000 × *g* for 4 h at 4 °C. Fractions were collected from the top and subsequently subjected to Western blotting analysis.

Western Blotting Analysis—For preparation of total cellular fraction, cells were collected into lysis buffer (65.8 mM Tris-HCl (pH 6.8), 26.3% glycerol, 2.1% SDS, 50 mM 2-mercaptoethanol, and Complete Mini protease inhibitor mixture) and lysed by incubating at 37 °C for 20 min. Proteins in either total cellular fractions, exosome fractions, or fractions from sucrose density gradient centrifugation were separated by SDS-PAGE and subsequently transferred electrophoretically to PVDF membrane. The blots were probed with the indicated primary antibodies followed either by Alexa Fluor 680-conjugated secondary antibodies for near-infrared fluorescence detection (LI-COR Odyssey) or by HRP-conjugated secondary antibodies for chemiluminescence detection. Unsaturated signals on the blot were captured and band intensities were quantified with ImageJ.

Immunoprecipitation—3 h after induction of GPRC5B-HA expression, cells were washed with DPBS (no calcium, no magnesium) and lysed in IP buffer (20 mM sodium phosphate (pH 7.2), 150 mM NaCl, 1 mM EDTA, 10% glycerol, 1% Triton X-100, and Complete Mini protease inhibitor mixture). After clearing the insoluble fraction, lysates were then incubated with anti-HA overnight followed by incubation with Protein G-Sepharose 4 Fast Flow (GE Healthcare) for 3 h. After washing five times with IP buffer, the captured immunoprecipitates were eluted with Laemmli sample buffer supplemented with a final concentration of 50 mM β-mercaptoethanol. For in-gel deglycosylation, GFP-tagged GPRC5B was immunoprecipitated with anti-GFP, and the immobilized GPRC5B-GFP was incubated with protein deglycosylation enzyme mixture (New England Biolabs) at 37 °C for 3 h prior to Western blotting analysis.

Cell Surface Biotinylation—Cell surface biotinylation was performed as described previously (62). Briefly, 0.8 mM membrane-impermeable EZ-Link Sulfo-NHS-SS biotin (pH 9.0) was used for labeling cell surface proteins, and biotinylated proteins were subsequently captured using NeutrAvidin-agarose (Thermo Scientific). Bound proteins were eluted with Laemmli sample buffer supplemented with 50 mM β-mercaptoethanol after extensive washing.

Statistical Analysis—All data were obtained from at least three independent experiments. Values are shown as mean ± S.E. Statistical significance was measured with Student's *t* test.

Author Contributions—S.-H. K. designed the research. S.-H. K., S. O., and M. N. performed experiments. S.-H. K., S. O., M. N., K. E. M., and J. H. L. analyzed the data. S.-H. K. and S. O. contributed to reagents and materials. S.-H. K., S. O., and J. H. L. wrote the paper.

Acknowledgments—We are grateful to Dr. Gerard Apodaca and members of the Mostov laboratory for helpful discussion. We thank Dr. Andrey Shaw for providing a CD2AP expression plasmid and Dr. Luke M. Judge for providing the 3xNLS-mKate-T2A-PuroR plasmid.

References

1. Colombo, M., Raposo, G., and Théry, C. (2014) Biogenesis, secretion, and intercellular interactions of exosomes and other extracellular vesicles. *Annu. Rev. Cell Dev. Biol.* **30,** 255–289
2. Raposo, G., and Stoorvogel, W. (2013) Extracellular vesicles: exosomes, microvesicles, and friends. *J. Cell Biol.* **200,** 373–383
3. Wakim, L. M., and Bevan, M. J. (2011) Cross-dressed dendritic cells drive memory $CD8^+$ T-cell activation after viral infection. *Nature* **471,** 629–632
4. Buschow, S. I., Nolte-'t Hoen, E. N., van Niel, G., Pols, M. S., ten Broeke, T., Lauwen, M., Ossendorp, F., Melief, C. J., Raposo, G., Wubbolts, R., Wauben, M. H., and Stoorvogel, W. (2009) MHC II in dendritic cells is targeted to lysosomes or T cell-induced exosomes via distinct multivesicular body pathways. *Traffic* **10,** 1528–1542
5. Gross, J. C., and Boutros, M. (2013) Secretion and extracellular space travel of Wnt proteins. *Curr. Opin. Genet. Dev.* **23,** 385–390
6. Gross, J. C., Chaudhary, V., Bartscherer, K., and Boutros, M. (2012) Active Wnt proteins are secreted on exosomes. *Nat. Cell Biol.* **14,** 1036–1045
7. Matusek, T., Wendler, F., Polès, S., Pizette, S., D'Angelo, G., Fürthauer, M., and Thérond, P. P. (2014) The ESCRT machinery regulates the secretion and long-range activity of Hedgehog. *Nature* **516,** 99–103
8. Gradilla, A.-C., González, E., Seijo, I., Andrés, G., Bischoff, M., González-Mendez, L., Sánchez, V., Callejo, A., Ibáñez, C., Guerra, M., Ortigão-Farias, J. R., Sutherland, J. D., González, M., Barrio, R., Falcón-Pérez, J. M., *et al.* (2014) Exosomes as Hedgehog carriers in cytoneme-mediated transport and secretion. *Nat. Commun.* **5,** 5649
9. Higginbotham, J. N., Demory Beckler, M., Gephart, J. D., Franklin, J. L., Bogatcheva, G., Kremers, G.-J., Piston, D. W., Ayers, G. D., McConnell, R. E., Tyska, M. J., and Coffey, R. J. (2011) Amphiregulin exosomes increase cancer cell invasion. *Curr. Biol.* **21,** 779–786
10. White, I. J., Bailey, L. M., Aghakhani, M. R., Moss, S. E., and Futter, C. E. (2006) EGF stimulates annexin 1-dependent inward vesiculation in a multivesicular endosome subpopulation. *EMBO J.* **25,** 1–12
11. Peinado, H., Alečković, M., Lavotshkin, S., Matei, I., Costa-Silva, B., Moreno-Bueno, G., Hergueta-Redondo, M., Williams, C., García-Santos, G., Ghajar, C., Nitadori-Hoshino, A., Hoffman, C., Badal, K., Garcia, B. A., Callahan, M. K., *et al.* (2012) Melanoma exosomes educate bone marrow progenitor cells toward a pro-metastatic phenotype through MET. *Nat. Med.* **18,** 883–891
12. Valadi, H., Ekström, K., Bossios, A., Sjöstrand, M., Lee, J. J., and Lötvall, J. O. (2007) Exosome-mediated transfer of mRNAs and microRNAs is a novel mechanism of genetic exchange between cells. *Nat. Cell Biol.* **9,** 654–659
13. Katritch, V., Cherezov, V., and Stevens, R. C. (2013) Structure-function of the G protein-coupled receptor superfamily. *Annu. Rev. Pharmacol. Toxicol.* **53,** 531–556
14. Keerthikumar, S., Gangoda, L., Liem, M., Fonseka, P., Atukorala, I., Ozcitti, C., Mechler, A., Adda, C. G., Ang, C.-S., and Mathivanan, S. (2015) Proteogenomic analysis reveals exosomes are more oncogenic than ectosomes. *Oncotarget* **6,** 15375–15396
15. Gonzales, P. A., Pisitkun, T., Hoffert, J. D., Tchapyjnikov, D., Star, R. A., Kleta, R., Wang, N. S., and Knepper, M. A. (2009) Large-scale proteomics and phosphoproteomics of urinary exosomes. *J. Am. Soc. Nephrol.* **20,** 363–379
16. Reinhardt, T. A., Sacco, R. E., Nonnecke, B. J., and Lippolis, J. D. (2013) Bovine milk proteome: quantitative changes in normal milk exosomes, milk fat globule membranes and whey proteomes resulting from *Staphylococcus aureus* mastitis. *J. Proteomics* **82,** 141–154
17. Hogan, M. C., Manganelli, L., Woollard, J. R., Masyuk, A. I., Masyuk, T. V., Tammachote, R., Huang, B. Q., Leontovich, A. A., Beito, T. G., Madden, B. J., Charlesworth, M. C., Torres, V. E., LaRusso, N. F., Harris, P. C., and Ward, C. J. (2009) Characterization of PKD protein-positive exosome-like vesicles. *J. Am. Soc. Nephrol.* **20,** 278–288
18. Kwon, S.-H., Liu, K. D., and Mostov, K. E. (2014) Intercellular transfer of GPRC5B via exosomes drives HGF-mediated outward growth. *Curr. Biol.* **24,** 199–204
19. Kurabayashi, N., Nguyen, M. D., and Sanada, K. (2013) The G protein-coupled receptor GPRC5B contributes to neurogenesis in the developing mouse neocortex. *Development* **140,** 4335–4346
20. Kim, Y.-J., Sano, T., Nabetani, T., Asano, Y., and Hirabayashi, Y. (2012) GPRC5B activates obesity-associated inflammatory signaling in adipocytes. *Sci. Signal.* **5,** ra85–ra85
21. Piper, R. C., and Katzmann, D. J. (2007) Biogenesis and function of multivesicular bodies. *Annu. Rev. Cell Dev. Biol.* **23,** 519–547
22. Hurley, J. H. (2015) ESCRTs are everywhere. *EMBO J.* **34,** 2398–2407
23. Baietti, M. F., Zhang, Z., Mortier, E., Melchior, A., Degeest, G., Geeraerts, A., Ivarsson, Y., Depoortere, F., Coomans, C., Vermeiren, E., Zimmermann, P., and David, G. (2012) Syndecan-syntenin-ALIX regulates the biogenesis of exosomes. *Nat. Cell Biol.* **14,** 677–685
24. Trajkovic, K., Hsu, C., Chiantia, S., Rajendran, L., Wenzel, D., Wieland, F., Schwille, P., Brügger, B., and Simons, M. (2008) Ceramide triggers budding of exosome vesicles into multivesicular endosomes. *Science* **319,** 1244–1247
25. Kajimoto, T., Okada, T., Miya, S., Zhang, L., and Nakamura, S. (2013) Ongoing activation of sphingosine 1-phosphate receptors mediates maturation of exosomal multivesicular endosomes. *Nat. Commun.* **4,** 2712
26. Hsu, C., Morohashi, Y., Yoshimura, S., Manrique-Hoyos, N., Jung, S., Lauterbach, M. A., Bakhti, M., Grønborg, M., Möbius, W., Rhee, J., Barr, F. A., and Simons, M. (2010) Regulation of exosome secretion by Rab35 and its GTPase-activating proteins TBC1D10A-C. *J. Cell Biol.* **189,** 223–232
27. Edwards, M., Zwolak, A., Schafer, D. A., Sept, D., Dominguez, R., and Cooper, J. A. (2014) Capping protein regulators fine-tune actin assembly dynamics. *Nat. Rev. Mol. Cell Biol.* **15,** 677–689
28. Reiterer, V., Nyfeler, B., and Hauri, H.-P. (2010) Role of the lectin VIP36 in post-ER quality control of human alpha1-antitrypsin. *Traffic* **11,** 1044–1055
29. Füllekrug, J., Scheiffele, P., and Simons, K. (1999) VIP36 localisation to the early secretory pathway. *J. Cell Sci.* **112,** 2813–2821
30. Doray, B., Ghosh, P., Griffith, J., Geuze, H. J., and Kornfeld, S. (2002) Cooperation of GGAs and AP-1 in packaging MPRs at the trans-Golgi network. *Science* **297,** 1700–1703
31. Bai, H., Doray, B., and Kornfeld, S. (2004) GGA1 interacts with the adaptor protein AP-1 through a WNSF sequence in its hinge region. *J. Biol. Chem.* **279,** 17411–17417
32. Taylor, D. D., Zacharias, W., and Gercel-Taylor, C. (2011) Exosome isolation for proteomic analyses and RNA profiling. *Methods Mol. Biol.* **728,** 235–246

33. de Gassart, A., Geminard, C., Fevrier, B., Raposo, G., and Vidal, M. (2003) Lipid raft-associated protein sorting in exosomes. *Blood* **102,** 4336–4344
34. Escola, J. M., Kleijmeer, M. J., Stoorvogel, W., Griffith, J. M., Yoshie, O., and Geuze, H. J. (1998) Selective enrichment of tetraspan proteins on the internal vesicles of multivesicular endosomes and on exosomes secreted by human B-lymphocytes. *J. Biol. Chem.* **273,** 20121–20127
35. Keerthikumar, S., Chisanga, D., Ariyaratne, D., Al Saffar, H., Anand, S., Zhao, K., Samuel, M., Pathan, M., Jois, M., Chilamkurti, N., Gangoda, L., and Mathivanan, S. (2016) ExoCarta: a web-based compendium of exosomal cargo. *J. Mol. Biol.* **428**, 688–692
36. Strauss, K., Goebel, C., Runz, H., Möbius, W., Weiss, S., Feussner, I., Simons, M., and Schneider, A. (2010) Exosome secretion ameliorates lysosomal storage of cholesterol in Niemann-Pick type C disease. *J. Biol. Chem.* **285,** 26279–26288
37. Géminard, C., De Gassart, A., Blanc, L., and Vidal, M. (2004) Degradation of AP2 during reticulocyte maturation enhances binding of hsc70 and Alix to a common site on TFR for sorting into exosomes. *Traffic* **5,** 181–193
38. Naslavsky, N., and Caplan, S. (2011) EHD proteins: key conductors of endocytic transport. *Trends Cell Biol.* **21,** 122–131
39. Donnelly, M. L., Hughes, L. E., Luke, G., Mendoza, H., ten Dam, E., Gani, D., and Ryan, M. D. (2001) The 'cleavage' activities of foot-and-mouth disease virus 2A site-directed mutants and naturally occurring "2A-like" sequences. *J. Gen. Virol.* **82,** 1027–1041
40. Szymczak, A. L., Workman, C. J., Wang, Y., Vignali, K. M., Dilioglou, S., Vanin, E. F., and Vignali, D. A. (2004) Correction of multi-gene deficiency *in vivo* using a single "self-cleaving" 2A peptide-based retroviral vector. *Nat. Biotechnol.* **22,** 589–594
41. Mali, P., Yang, L., Esvelt, K. M., Aach, J., Guell, M., DiCarlo, J. E., Norville, J. E., and Church, G. M. (2013) RNA-guided human genome engineering via Cas9. *Science* **339,** 823–826
42. Cong, L., Ran, F. A., Cox, D., Lin, S., Barretto, R., Habib, N., Hsu, P. D., Wu, X., Jiang, W., Marraffini, L. A., and Zhang, F. (2013) Multiplex genome engineering using CRISPR/Cas systems. *Science* **339,** 819–823
43. Engelsberg, A., Hermosilla, R., Karsten, U., Schülein, R., Dörken, B., and Rehm, A. (2003) The Golgi protein RCAS1 controls cell surface expression of tumor-associated *O*-linked glycan antigens. *J. Biol. Chem.* **278,** 22998–23007
44. Zhou, H., Pisitkun, T., Aponte, A., Yuen, P. S., Hoffert, J. D., Yasuda, H., Hu, X., Chawla, L., Shen, R.-F., Knepper, M. A., and Star, R. A. (2006) Exosomal Fetuin-A identified by proteomics: a novel urinary biomarker for detecting acute kidney injury. *Kidney Int.* **70,** 1847–1857
45. Rouka, E., Simister, P. C., Janning, M., Kumbrink, J., Konstantinou, T., Muniz, J. R., Joshi, D., O'Reilly, N., Volkmer, R., Ritter, B., Knapp, S., von Delft, F., Kirsch, K. H., and Feller, S. M. (2015) Differential recognition preferences of the three Src homology 3 (SH3) domains from the adaptor CD2-associated protein (CD2AP), and direct association with Ras and Rab interactor 3 (RIN3). *J. Biol. Chem.* **290,** 25275–25292
46. Usami, Y., Popov, S., and Göttlinger, H. G. (2007) Potent rescue of human immunodeficiency virus type 1 late domain mutants by ALIX/AIP1 depends on its CHMP4 binding site. *J. Virol.* **81,** 6614–6622
47. Burd, C., and Cullen, P. J. (2014) Retromer: a master conductor of endosome sorting. *Cold Spring Harb. Perspect. Biol.* **6,** a016774
48. Gallon, M., and Cullen, P. J. (2015) Retromer and sorting nexins in endosomal sorting. *Biochem Soc. Trans.* **43,** 33–47
49. Seaman, M. N., Gautreau, A., and Billadeau, D. D. (2013) Retromer-mediated endosomal protein sorting: all WASHed up! *Trends Cell Biol.* **23,** 522–528
50. Gokool, S., Tattersall, D., and Seaman, M. N. (2007) EHD1 interacts with retromer to stabilize SNX1 tubules and facilitate endosome-to-Golgi retrieval. *Traffic* **8,** 1873–1886
51. Mukadam, A. S., and Seaman, M. N. (2015) Retromer-mediated endosomal protein sorting: the role of unstructured domains. *FEBS Lett.* **589,** 2620–2626
52. Zhang, J., Naslavsky, N., and Caplan, S. (2012) EHDs meet the retromer: complex regulation of retrograde transport. *Cell. Logist.* **2,** 161–165
53. Korkut, C., Ataman, B., Ramachandran, P., Ashley, J., Barria, R., Gherbesi, N., and Budnik, V. (2009) Trans-synaptic transmission of vesicular Wnt signals through Evi/Wntless. *Cell* **139,** 393–404
54. Yang, P.-T., Lorenowicz, M. J., Silhankova, M., Coudreuse, D. Y., Betist, M. C., and Korswagen, H. C. (2008) Wnt signaling requires retromer-dependent recycling of MIG-14/Wntless in Wnt-producing cells. *Dev Cell.* **14,** 140–147
55. Belenkaya, T. Y., Wu, Y., Tang, X., Zhou, B., Cheng, L., Sharma, Y. V., Yan, D., Selva, E. M., and Lin, X. (2008) The retromer complex influences Wnt secretion by recycling wntless from endosomes to the trans-Golgi network. *Dev Cell.* **14,** 120–131
56. Port, F., Kuster, M., Herr, P., Furger, E., Bänziger, C., Hausmann, G., and Basler, K. (2008) Wingless secretion promotes and requires retromer-dependent cycling of Wntless. *Nat Cell Biol.* **10,** 178–185
57. Silhankova, M., Port, F., Harterink, M., Basler, K., and Korswagen, H. C. (2010) Wnt signalling requires MTM-6 and MTM-9 myotubularin lipid-phosphatase function in Wnt-producing cells. *EMBO J.* **29,** 4094–4105
58. Harterink, M., Port, F., Lorenowicz, M. J., McGough, I. J., Silhankova, M., Betist, M. C., van Weering, J. R., van Heesbeen, R. G., Middelkoop, T. C., Basler, K., Cullen, P. J., and Korswagen, H. C. (2011) A SNX3-dependent retromer pathway mediates retrograde transport of the Wnt sorting receptor Wntless and is required for Wnt secretion. *Nat. Cell Biol.* **13,** 914–923
59. Shirakabe, K., Hattori, S., Seiki, M., Koyasu, S., and Okada, Y. (2011) VIP36 protein is a target of ectodomain shedding and regulates phagocytosis in macrophage Raw 264.7 cells. *J. Biol. Chem.* **286,** 43154–43163
60. Gibson, D. G., Young, L., Chuang, R.-Y., Venter, J. C., Hutchison, C. A., 3rd, and Smith, H. O. (2009) Enzymatic assembly of DNA molecules up to several hundred kilobases. *Nat. Methods* **6,** 343–345
61. Oh, S., Flynn, R. A., Floor, S. N., Purzner, J., Martin, L., Do, B. T., Schubert, S., Vaka, D., Morrissy, S., Li, Y., Kool, M., Hovestadt, V., Jones, D. T., Northcott, P. A., Risch, T., *et al.* (2016) Medulloblastoma-associated DDX3 variant selectively alters the translational response to stress. *Oncotarget* **7,** 28169–28182
62. Kwon, S.-H., and Guggino, W. B. (2004) Multiple sequences in the C terminus of MaxiK channels are involved in expression, movement to the cell surface, and apical localization. *Proc. Natl. Acad. Sci. U.S.A.* **101,** 15237–15242